



# Generation of transverse photo-induced voltage in plasmonic metasurfaces of triangle holes

MARJAN AKBARI,<sup>1</sup> JIE GAO,<sup>1,2</sup> AND XIAODONG YANG<sup>1,3</sup>

<sup>1</sup>Department of Mechanical and Aerospace Engineering, Missouri University of Science and Technology, Rolla, MO, 65409, USA

<sup>2</sup>gaojie@mst.edu

<sup>3</sup>yangxia@mst.edu

**Abstract:** We experimentally and numerically demonstrate the transverse electrical response produced by circularly-polarized light with normal incidence observed as transverse photo-induced voltage across the plasmonic metasurface made of triangle holes. The measured transverse photo-induced voltage is consistent with the calculated acting force on electrons in the metasurface by using the Maxwell's stress tensor. The polarity of voltage reverses as the incident spin (light helicity) switches from right-handed circular polarization to left-handed circular polarization. The origin of the spin-dependent voltage sign is the broken symmetries of the electric and magnetic fields in the triangle hole due to the opposite circular polarizations. The demonstrated results open up many opportunities in further investigating the second-order nonlinear optical effects of metamaterials and metasurfaces, and developing applications in high-speed photodetectors, polarimeters, and optical sensors.

© 2018 Optical Society of America under the terms of the [OSA Open Access Publishing Agreement](#)

## 1. Introduction

By the interaction of a light source with conductive material such as a metal film, electromagnetic fields of light beam will apply Lorentz force on the conduction electrons, resulting in photo-induced voltage (PIV) across the film. In this case, manipulating the amplitude and sign of the produced voltage by wavelength, polarization or incidence angle is the main purpose, which is of interest for the development of fast response photodetectors and sensors. Such force can be estimated by using momentum conservation, that is, the momentum from photons transfers to the free carriers of the material and this effect manifests itself as a pulsed voltage (or emf) signal [1]. PIV proportional to the light intensity can be observed along and/or perpendicular to the incident plane, depending on the polarization states. We refer the phenomena to be longitudinal photo-induced voltage (LPIV) or transverse photo-induced voltage (TPIV) effects, respectively. This phenomenon has been explained as photon drag effect in semiconductors, which was first experimentally observed with the CO<sub>2</sub> laser excitation on holes and electrons in bulk germanium crystals [2,3]. Semiconductors such as Ge, Si, GaAs and Te have already found applications in photon drag detectors [4].

The photo-induced dc electric currents caused by different mechanisms, including photogalvanic effect, ratchet effect, and photon drag effect, have been previously investigated in various material systems. Linear and circular photogalvanic effects have been reported for semiconductor structures with periodic arrays of asymmetric triangular antidots [5] and semidisks [6,7], wurtzite GaN/AlGaIn heterojunctions [8], and 3D topological insulators such as Bi<sub>2</sub>Se<sub>3</sub>, Sb<sub>2</sub>Te<sub>3</sub>, Bi<sub>2</sub>Te<sub>3</sub> and (Bi<sub>1-x</sub>Sb<sub>x</sub>)<sub>2</sub>Te<sub>3</sub> [9–11]. Linear and circular electronic ratchet effects have been observed in semiconductor quantum wells with lateral asymmetric grating and graphene with lateral double-grating-gate structures [12,13]. Linear and helicity-driven plasmonic ratchet effects have also been studied in field-effect transistor structures with asymmetric grating gates [14,15]. In particular, the generation of circular photocurrents has been reported due to different mechanisms, such as circular photon drag effects in GaAs/AlGaAs quantum well structures [16], circular ac Hall effect in graphene [17], circular

photogalvanic effects in topological insulators, quantum wells and graphene [9,18,19], and circular electronic and plasmonic ratchet effects in low-dimensional semiconductor structures with lateral asymmetric periodic potentials [12–15].

In principle, photon drag effect is also expected for surface of metals [20]. The photon drag effect induced current in metals without surface plasmon resonance has been described using the equation of motion for the electrons with a hydrodynamic model [21]. This effect is significant in semiconductors [22] but very weak in bulk metals [23]. The surface plasmon enhanced photon drag effect in a thin gold film has been reported, where the observed PIV depends on the incidence angle and polarization of light [24]. Subwavelength structures in photonic crystals and metamaterials with plasmonic resonances can further enhance the PIV observed in semiconductors or metals [25–28], and usually TPIV is observed with obliquely incident light for symmetric structures such as gratings and circular holes [28–33]. When the laser beam is obliquely incident to the sample surface, the symmetry in the system is broken and TPIV is generated for non-zero incident angles [27,28]. For the photonic crystal slab with circular holes [27], the calculated electric field distribution shows symmetry breaking of the fields with obliquely incident light, which can explain the TPIV generation and its sign change by switching the incident spin (here spin is used for light helicity). For the plasmonic crystal with nanovoids [33], the mechanism of TPIV is explained as a gradient force arising from asymmetric field hotspots around nanovoids with obliquely incident light, which results in reversed gradient forces or voltages for light with opposite circular polarizations. Recently, gold-glass-gold three-layer metasurface has been numerically proposed to realize TPIV by exciting magnetic resonance with normally incident light due to the asymmetric antenna structures [34].

In this paper, the gold single-layer plasmonic metasurfaces made of periodic triangle holes are designed to produce spin-dependent TPIV with normally incident light, by breaking the symmetry of electromagnetic field in the asymmetric triangle structure for right-handed and left-handed circular polarizations (RCP and LCP). The measured TPIV agrees well with the calculated Lorentz force on electrons in the metasurface. It is also demonstrated that the polarity of TPIV reverses as the incident circular polarization switches. It is shown that the spin-dependent TPIV sign is due to the symmetry breaking of the electric and magnetic fields in the asymmetric triangle hole. These results offer many possibilities in future studies of the second-order nonlinear optical effects in metasurfaces and the applications in integrated photodetectors, polarimeters, and optical sensors.

## 2. Design of plasmonic metasurface

Figure 1(a) shows the design of plasmonic metasurfaces to generate TPIV. A layer of gold film of 50 nm thickness is deposited on glass substrate by electron beam evaporation process. The metasurface is made of the square lattice of isosceles triangle nanoholes with base and height of 250 nm and period of 370 nm. The permittivity of glass is a constant 2.25 and the permittivity of gold is from the Drude model. The triangle base is along the  $y$  axis which allows the symmetry breaking of electromagnetic field respect to the  $x$  axis within the square unit cell; therefore TPIV is the voltage across the structure along the  $y$  axis. Figure 1(b) shows the simulated distributions of electric and magnetic fields on the  $x$ - $y$  plane inside the gold layer for LCP and RCP incident light at the plasmonic resonance of 800 nm. Both electric and magnetic fields display symmetry breaking respect to the  $x$  axis with the enhanced hotspots in opposite locations in each triangle hole, which results in opposite Lorentz force on the electrons in the gold metasurface film. The metasurface sample with size of 50  $\mu\text{m}$  by 50  $\mu\text{m}$  including 135 triangle holes is fabricated with focused ion beam (FIB) milling, and Fig. 2(a) shows the SEM image of the metasurface. Figure 2(b) shows the measured and simulated transmission, reflection, and absorption spectra of the metasurface for normally incident LCP light. The absorption is large for wavelength between 750 and 850 nm due to the plasmonic resonance so that the enhanced TPIV is expected.

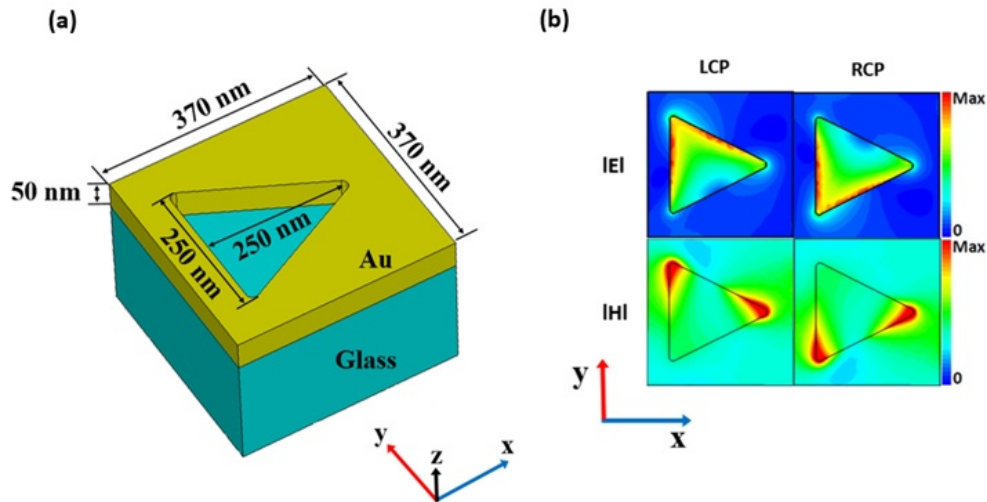


Fig. 1. (a) Schematic of the designed plasmonic metasurface with triangle holes. (b) Simulated distributions of the electric and magnetic fields on the  $x$ - $y$  plane at the middle plane.

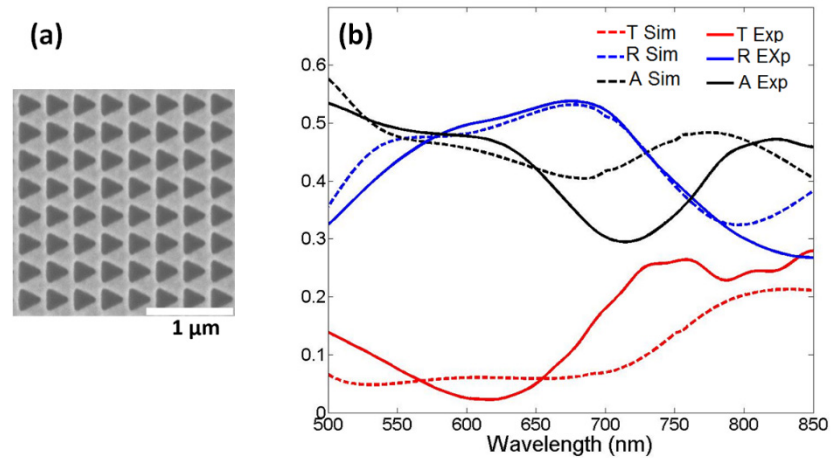


Fig. 2. (a) SEM image of the metasurface sample. (b) Measured and simulated transmission (T), reflection (R), and absorption (A) spectra of the metasurface for normally incident LCP light.

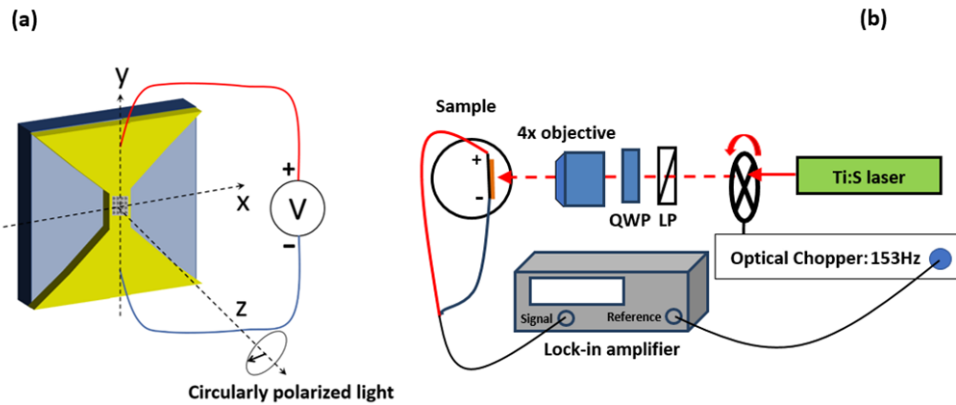


Fig. 3. (a) Sample in the transverse configuration with connected electrodes. (b) Experimental setup for measuring TPIV across the metasurface.

### 3. Observation of transverse photo-induced voltage

In order to measure TPIV across the metasurface sample, two electrodes in the gold film are connected perpendicular to the  $x$ - $z$  plane, which is called the transverse configuration, as shown in Fig. 3(a). A schematic diagram of the experimental setup is shown in Fig. 3(b). A tunable Ti:Sapphire laser is used as the light source. An optical chopper with 153 Hz is utilized to modulate the laser signal. A linear polarizer and a quarter wave plate in the setup control the circular polarization of the incident light. A 4x objective lens is employed to focus the light on the sample with normal incidence. The electrical signal is sent to a lock-in amplifier for measuring the TPIV as functions of optical power, wavelength and polarization. Figure 4(a) plots the dependence of the measured TPIV on the power of the RCP and LCP incident light at the fixed wavelength of 800 nm, showing that photon drag effect has a linear relation with the laser excitation power, which is different from the second-harmonic generation process with quadratic dependence on the pump power. Next, TPIV is measured with a fixed power of 10 mW for 750-850 nm wavelength range. As shown in Fig. 4(b), TPIV around 0.03  $\mu$ V is obtained, giving the external responsivity of 3 nV/mW. The polarity of TPIV reverses as the incident circular polarization is switched from RCP to LCP, showing the spin-dependent TPIV with normally incident light.

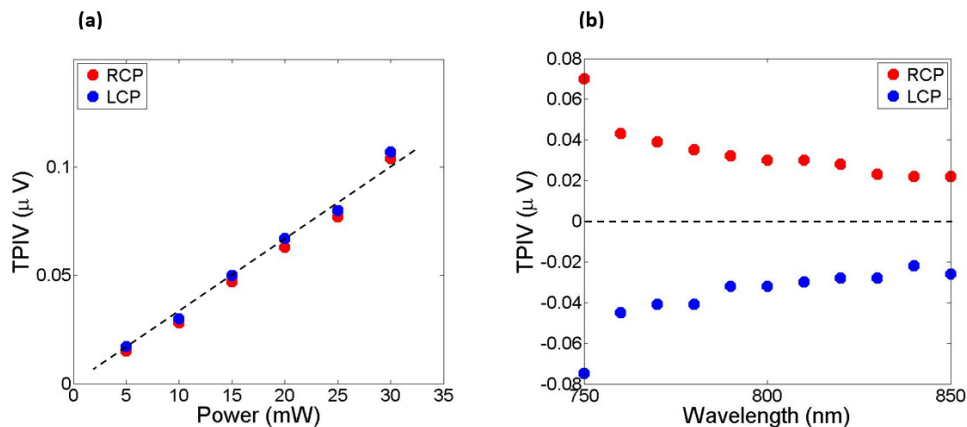


Fig. 4. (a) Dependence of the measured TPIV on the power of the RCP and LCP incident light at the wavelength of 800 nm. The dashed line represents a linear fit to the experimental data. (b) Measured TPIV for RCP and LCP light with a fixed power of 10 mW for 750-850 nm wavelength range.

In order to explain the observed TPIV signal, the Lorentz force applied on the free electrons in the metasurface layer is further simulated according to the symmetry-broken electric and magnetic fields in the triangle hole structure [34]. The PIV with  $V_i$  ( $i = x$  and  $y$ , is direction of the generated voltage) can be estimated in term of the force  $F_i$  as

$$V_i = \frac{L \langle F_i \rangle}{-e \rho \Omega} \quad (1)$$

Here  $L$  is the length of sample along the  $i$  axis.  $\langle F_i \rangle$  is total averaged force on the free electrons,  $e$  is charge of free electron,  $\rho$  is the volume density of free electrons in the gold film and  $\Omega$  is the total volume of gold in the sample. For TPIV ( $V_y$ ) studied here,

$$V_y = \frac{L \langle F_y \rangle}{-e \rho \Omega} \quad (2)$$

And the force  $\langle F_i \rangle$  is calculated by integrating the Maxwell's stress tensor  $\langle T_{ij} \rangle$  around the gold film [35],

$$\langle F_i \rangle = \oiint_S \langle T_{ij} \rangle n_j dS \quad (3)$$

$\langle F_y \rangle$  is calculated from the integration along the top and down surfaces around the gold film,

$$\langle F_y \rangle = \oiint_S \langle T_{yz} \rangle n_z dS = \int_{Su} \langle T_{yz} \rangle n_z dS - \int_{Sd} \langle T_{yz} \rangle n_z dS \quad (4)$$

$Su$  and  $Sd$  are top and down  $x$ - $y$  planes in the air and glass, respectively. The elements of the Maxwell's stress tensor are related to the electric and magnetic field,

$$\langle T_{ij} \rangle = \frac{1}{2} Re \left[ \epsilon \epsilon_0 \left( E_i E_j^* - \frac{1}{2} \delta_{ij} E^2 \right) + \mu \mu_0 \left( H_i H_j^* - \frac{1}{2} \delta_{ij} H^2 \right) \right] \quad (5)$$

$\epsilon$  and  $\mu$  are relative permittivity and permeability of the dielectrics (air or glass), respectively. According to Eq. (4), only the term of  $\langle T_{yz} \rangle$  is necessary in order to estimate  $\langle F_y \rangle$ ,

$$\langle T_{yz} \rangle = \frac{1}{2} Re \left[ \epsilon \epsilon_0 (E_y E_z^*) + \mu \mu_0 (H_y H_z^*) \right] \quad (6)$$

Figure 5 shows the calculated TPIV ( $V_y$ ) with RCP and LCP normally incident light as a function of wavelength, which is consistent with the measured TPIV from the sample in Fig. 4(b).

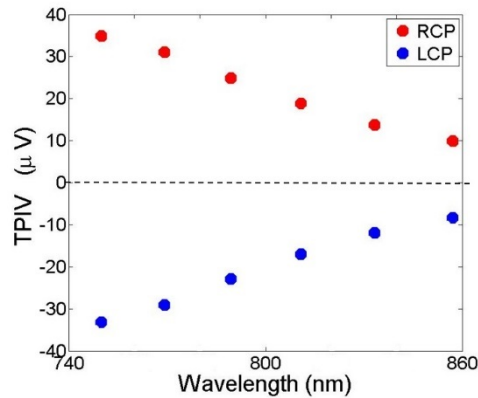


Fig. 5. Calculated TPIV across the metasurface as a function of wavelength for RCP and LCP normally incident light with the fixed power.

As seen in Fig. 1(b), the hotspots of electromagnetic fields around the corner of the triangle hole are shifted as the circular polarization is switched. This shift indicates a change in momentum exchange which is the effect of coupling between spin angular momentum of incident light with orbital angular momentum of surface plasmons [33,36]. Compared to the three-layer metasurface proposed to calculate TPIV across the bottom continuous metallic film in [34], the single-layer metasurface structure studied here supports TPIV across the metasurface layer with air holes embedded, which has simpler design and is easier to fabricate. The symmetry-broken electric and magnetic fields in the triangle hole structure enables the spin-dependent TPIV which is proven with both experimental and simulated results.

The helicity-dependent photovoltages can be caused by different mechanisms such as photogalvanic effect, photon drag effect, and ratchet effect. The ratchet photocurrent is usually generated in low-dimensional semiconductor structures with lateral noncentrosymmetric periodic potentials. The photogalvanic effect requires the lack of inversion symmetry, and the photogalvanic current is determined by the in-plane orientation of electric field and is insensitive to the light propagation direction [10,11]. On the contrary, the photon drag effect does not require the lack of inversion symmetry and it is proportional to the photon wave vector  $\mathbf{q}$  due to the light momentum transfer to charged carriers. As a result, the photogalvanic current remains unchanged at  $\mathbf{q} \rightarrow -\mathbf{q}$  inversion for both front and back illuminations at normal incidence, but the sign of the photon drag current will be flipped with the reversed light propagation direction, which provides an approach to distinguish the photogalvanic effect and the photon drag effect from each other [11]. At oblique incidence with the incident angle less than  $\pm 30^\circ$ , it has been observed that the photogalvanic current just slightly decreases with the increased incident angle, however, the photon drag current dramatically changes the amplitude related to the in-plane component of the photon wave vector [11,16]. Figure 6 shows the dependence of the measured TPIV on the incident angle  $\theta$  from  $-15^\circ$  to  $+15^\circ$  for RCP and LCP light with a fixed power of 10 mW at the wavelength of 800 nm. It shows that the measured TPIV signal decreases significantly with the increased incident angle and reaches the maximum value at normal incidence, manifesting the feature of photon drag effect rather than photogalvanic effect. The variation of incident angle affects the in-plane component of the photon wave vector and thus changes the generated photon drag current across the metasurface. It is known that in symmetric structures the TPIV has zero value at normal incidence and the photovoltage is anti-symmetric as a function of the incident angle [25]. However, here the TPIV has the maximum non-zero value at normal incidence due to the large in-plane photon wave vector generated by the asymmetric triangle holes. In

addition, the TPIV has an asymmetric profile as a function of the incident angle, indicating the symmetry-breaking effects from the triangle hole unit cell on the in-plane photon wave vector. The TPIV signals at positive incident angles are stronger than those at negative incident angles due to the interplay between the asymmetric triangle structure and the obliquely incident light. It is also noted that the sign of TPIV will keep unchanged as the incident angle varies.

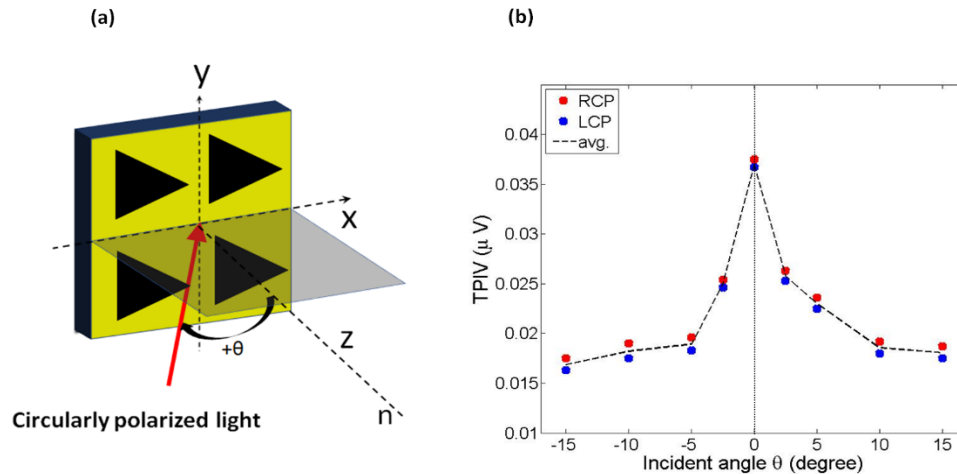


Fig. 6. (a) The oblique incidence setup with the incident angle  $\theta$ . (b) The dependence of the measured TPIV on the incident angle  $\theta$  from  $-15^\circ$  to  $+15^\circ$  for RCP and LCP light with a fixed power of 10 mW at the wavelength of 800 nm. The dashed curve represents the averaged TPIV between two circular polarizations.

The symmetry of the triangle hole unit cell can be further analyzed to reveal the TPIV generation at normal incidence. For the equilateral triangle hole having  $C_{3v}$  point group symmetry, the circular photon drag current will vanish at normal incidence. However, the isosceles triangle hole with  $C_s$  symmetry used in the current work will allow the helicity-dependent photon drag current at normal incidence. In addition, the entire square unit cell embedded with the isosceles triangle hole also presents  $C_s$  symmetry, which further enables the circular photocurrent at normal incidence.

#### 4. Conclusion

The plasmonic metasurfaces made of periodic triangle holes have been studied to generate spin-dependent transverse photo-induced voltage with normally incident light, by breaking the symmetry of electromagnetic field in the triangle hole structure for circularly polarized light. The transverse photo-induced voltage is further estimated by the calculated Lorentz force on electrons in the metasurface film. We have demonstrated that the sign of transverse photo-induced voltage depends on the incident spin. It is explained that the spin-dependent voltage polarity is due to the symmetry breaking of the electric and magnetic fields in the triangle hole structure. Our results will advance many metasurface-based optoelectronic applications in photodetectors, polarimeters, optical sensing, and optical imaging.

#### Funding

National Science Foundation (NSF) (ECCS-1653032, DMR-1552871); Office of Naval Research (ONR) (N00014-16-1-2408).

#### Acknowledgments

The authors acknowledge the facility support from the Materials Research Center at Missouri S&T. The authors also thank Yuchao Zhang for the FIB milling of gold film.

## References

1. G. M. Mikheev, V. M. Styapshin, P. A. Obraztsov, E. A. Khestanova, and S. V. Garnov, "Effect of laser light polarization on the dc photovoltage response of nongraphite films," *Quantum Electron.* **40**(5), 425–430 (2010).
2. A. M. Danishevskii, A. A. Kastalskii, S. M. Ryvkin, and I. D. Yarashetskii, "Dragging of free carriers by photons in direct interband transitions in semiconductors," *Sov. Phys. JETP* **31**, 292–295 (1970).
3. A. F. Gibson, M. F. Kimmitt, and A. C. Walker, "Photon drag in germanium," *Appl. Phys. Lett.* **17**(2), 75–77 (1970).
4. J. Shirafuji and Y. Inuishi, "Photon drag effect in semiconductors," *Oyobuturi* **44**, 838–851 (1975).
5. A. Lorke, S. Wimmer, B. Jäger, J. P. Kotthaus, W. Wegscheider, and M. Bichler, "Far-infrared and transport properties of antidot arrays with broken symmetry," *Physica B* **249–251**, 312–316 (1998).
6. A. D. Chepelianskii, M. V. Entin, L. I. Magarill, and D. L. Shepelyansky, "Photogalvanic current in artificial asymmetric nanostructures," *Eur. Phys. J. B* **56**(4), 323–333 (2007).
7. A. D. Chepelianskii, M. V. Entin, L. I. Magarill, and D. L. Shepelyansky, "Theory of Photogalvanic effect in asymmetric nanostructure arrays," *Physica E* **40**(5), 1264–1266 (2008).
8. W. Weber, L. E. Golub, S. N. Danilov, J. Karch, C. Reitmaier, B. Wittmann, V. V. Bel'kov, E. L. Ivchenko, Z. D. Kvon, N. Q. Vinh, A. F. G. van der Meer, B. Murdin, and S. D. Ganichev, "Quantum ratchet effects induced by terahertz radiation in GaN-based two-dimensional structures," *Phys. Rev. B* **77**(24), 245304 (2008).
9. J. W. McIver, D. Hsieh, H. Steinberg, P. Jarillo-Herrero, and N. Gedik, "Control over topological insulator photocurrents with light polarization," *Nat. Nanotechnol.* **7**(2), 96–100 (2012).
10. P. Olbrich, L. E. Golub, T. Herrmann, S. N. Danilov, H. Plank, V. V. Bel'kov, G. Mussler, Ch. Weyrich, C. M. Schneider, J. Kampmeier, D. Grützmacher, L. Plucinski, M. Eschbach, and S. D. Ganichev, "Room-temperature high-frequency transport of Dirac fermions in epitaxially grown Sb<sub>2</sub>Te<sub>3</sub>- and Bi<sub>2</sub>Te<sub>3</sub>-based topological insulators," *Phys. Rev. Lett.* **113**(9), 096601 (2014).
11. H. Plank, L. E. Golub, S. Bauer, V. V. Bel'kov, T. Herrmann, P. Olbrich, M. Eschbach, L. Plucinski, C. M. Schneider, J. Kampmeier, M. Lanus, G. Mussler, D. Grützmacher, and S. D. Ganichev, "Photon drag effect in (Bi<sub>1-x</sub>Sbx)<sub>2</sub>Te<sub>3</sub> three-dimensional topological insulators," *Phys. Rev. B* **93**(12), 125434 (2016).
12. P. Olbrich, E. L. Ivchenko, R. Ravash, T. Feil, S. D. Danilov, J. Allerdings, D. Weiss, D. Schuh, W. Wegscheider, and S. D. Ganichev, "Ratchet effects induced by terahertz radiation in heterostructures with a lateral periodic potential," *Phys. Rev. Lett.* **103**(9), 090603 (2009).
13. P. Olbrich, J. Kamann, M. König, J. Munzert, L. Tutsch, J. Eroms, D. Weiss, M.-H. Liu, L. E. Golub, E. L. Ivchenko, V. V. Popov, D. V. Fateev, K. V. Mashinsky, F. Fromm, Th. Seyller, and S. D. Ganichev, "Terahertz ratchet effects in graphene with a lateral superlattice," *Phys. Rev. B* **93**(7), 075422 (2016).
14. V. V. Popov, D. V. Fateev, T. Otsuji, Y. M. Meziani, D. Coquillat, and W. Knap, "Plasmonic terahertz detection by a double-grating-gate field-effect transistor structure with an asymmetric unit cell," *Appl. Phys. Lett.* **99**(24), 243504 (2011).
15. I. V. Rozhansky, V. Yu. Kachorovskii, and M. S. Shur, "Helicity-driven ratchet effect enhanced by plasmons," *Phys. Rev. Lett.* **114**(24), 246601 (2015).
16. H. Diehl, V. A. Shalygin, V. V. Bel'kov, Ch. Hoffmann, S. N. Danilov, T. Herrle, S. A. Tarasenko, D. Schuh, Ch. Gerl, W. Wegscheider, W. Prettl, and S. D. Ganichev, "Spin photocurrents in (110)-grown quantum well structures," *New J. Phys.* **9**(9), 349 (2007).
17. J. Karch, P. Olbrich, M. Schmalzbauer, C. Zoth, C. Brinsteiner, M. Fehrenbacher, U. Wurstbauer, M. M. Glazov, S. A. Tarasenko, E. L. Ivchenko, D. Weiss, J. Eroms, R. Yakimova, S. Lara-Avila, S. Kubatkin, and S. D. Ganichev, "Dynamic Hall effect driven by circularly polarized light in a graphene layer," *Phys. Rev. Lett.* **105**(22), 227402 (2010).
18. S. D. Ganichev, E. L. Ivchenko, S. N. Danilov, J. Eroms, W. Wegscheider, D. Weiss, and W. Prettl, "Conversion of spin into directed electric current in quantum wells," *Phys. Rev. Lett.* **86**(19), 4358–4361 (2001).
19. C. Jiang, V. A. Shalygin, V. Yu. Panevin, S. N. Danilov, M. M. Glazov, S. Rositsa Yakimova, L. Avila, S. Kubatkin, and S. D. Ganichev, "Helicity-dependent photocurrents in graphene layers excited by mid infrared radiation of a CO<sub>2</sub> laser," *Phys. Rev. B* **84**, 125429 (2011).
20. J. E. Goff and W. L. Schaich, "Theory of the photon-drag effect in simple metals," *Phys. Rev. B* **61**(15), 10471–10477 (2000).
21. J. E. Goff and W. L. Schaich, "Hydrodynamic theory of photon drag," *Phys. Rev. B* **56**(23), 15421–15430 (1997).
22. S. Luryi, "Photon-drag effect in intersubband absorption by a two-dimensional electron gas," *Phys. Rev. Lett.* **58**(21), 2263–2266 (1987).
23. V. L. Gurevich and R. Laiho, "Photomagnetism of metals, first observation of dependence on polarization of light," *Phys. Solid State* **42**(10), 1807–1812 (2000).
24. A. S. Vengurlekar and T. Ishihara, "Surface plasmon enhanced photon drag in metal films," *Appl. Phys. Lett.* **87**(9), 091118 (2005).
25. T. Hatano, B. Nishikawa, M. Iwanaga, and T. Ishihara, "Optical rectification effect in 1D metallic photonic crystal slabs with asymmetric unit cell," *Opt. Express* **16**(11), 8236–8241 (2008).
26. T. Ishihara, "Optical response of semiconductor and metal-embedded photonic crystal slabs," *Phys. Status Solidi, A Appl. Res.* **201**(3), 398–404 (2004).

27. T. Hatano, T. Ishihara, S. G. Tikhodeev, and N. A. Gippius, "Transverse photovoltage induced by circularly polarized light," *Phys. Rev. Lett.* **103**(10), 103906 (2009).
28. H. Kurosawa and T. Ishihara, "Surface plasmon drag effect in a dielectrically modulated metallic thin film," *Opt. Express* **20**(2), 1561–1574 (2012).
29. N. Noginova, V. Rono, F. J. Bezares, and J. D. Caldwell, "Plasmon drag effect in metal nanostructures," *New J. Phys.* **15**(11), 113061 (2013).
30. M. M. Glazov and S. D. Ganichev, "High frequency electric field induced nonlinear effects in graphene," *Phys. Rep.* **535**(3), 101–138 (2014).
31. M. Akbari, M. Onoda, and T. Ishihara, "Photo-induced voltage in nano-porous gold thin film," *Opt. Express* **23**(2), 823–832 (2015).
32. M. Akbari and T. Ishihara, "Polarization dependence of transverse photo-induced voltage in gold thin film with random nanoholes," *Opt. Express* **25**(3), 2143–2152 (2017).
33. N. V. Proscia, M. Moccarme, R. Chang, I. Kretzschmar, V. M. Menon, and L. T. Vuong, "Control of photo-induced voltages in plasmonic crystals via spin-orbit interactions," *Opt. Express* **24**(10), 10402–10411 (2016).
34. Q. Bai, "Manipulating photoinduced voltage in metasurface with circularly polarized light," *Opt. Express* **23**(4), 5348–5356 (2015).
35. J. D. Jackson, *Classical Electrodynamics*, 3rd ed. (John Wiley & Sons, 1999).
36. Y. Gorodetski, N. Shitrit, I. Bretner, V. Kleiner, and E. Hasman, "Observation of optical spin symmetry breaking in nanoapertures," *Nano Lett.* **9**(8), 3016–3019 (2009).

---

## References

1. G. M. Mikheev, V. M. Styapshin, P. A. Obraztsov, E. A. Khestanova, and S. V. Garnov, "Effect of laser light polarization on the dc photovoltage response of nongraphite films," *Quantum Electron.* **40**(5), 425–430 (2010).
2. A. M. Danishevskii, A. A. Kastalskii, S. M. Ryvkin, and I. D. Yarashetskii, "Dragging of free carriers by photons in direct interband transitions in semiconductors," *Sov. Phys. JETP* **31**, 292–295 (1970).
3. A. F. Gibson, M. F. Kimmitt, and A. C. Walker, "Photon drag in germanium," *Appl. Phys. Lett.* **17**(2), 75–77 (1970).
4. J. Shirafuji and Y. Inuishi, "Photon drag effect in semiconductors," *Oyobuturi* **44**, 838–851 (1975).
5. A. Lorke, S. Wimmer, B. Jager, J. P. Kotthaus, W. Wegscheider, and M. Bichler, "Far-infrared and transport properties of antidot arrays with broken symmetry," *Physica B* **249-251**, 312–316 (1998).
6. A. D. Chepelianskii, M. V. Entin, L. I. Magarill, and D. L. Shepelyansky, "Photogalvanic current in artificial asymmetric nanostructures," *Eur. Phys. J. B* **56**(4), 323–333 (2007).
7. A. D. Chepelianskii, M. V. Entin, L. I. Magarill, and D. L. Shepelyansky, "Theory of Photogalvanic effect in asymmetric nanostructure arrays," *Physica E* **40**(5), 1264–1266 (2008).
8. W. Weber, L. E. Golub, S. N. Danilov, J. Karch, C. Reitmaier, B. Wittmann, V. V. Bel'kov, E. L. Ivchenko, Z. D. Kvon, N. Q. Vinh, A. F. G. van der Meer, B. Murdin, and S. D. Ganichev, "Quantum ratchet effects induced by terahertz radiation in GaN-based two-dimensional structures," *Phys. Rev. B* **77**(24), 245304 (2008).
9. J. W. McIver, D. Hsieh, H. Steinberg, P. Jarillo-Herrero, and N. Gedik, "Control over topological insulator photocurrents with light polarization," *Nat. Nanotechnol.* **7**(2), 96–100 (2012).
10. P. Olbrich, L. E. Golub, T. Herrmann, S. N. Danilov, H. Plank, V. V. Bel'kov, G. Mussler, Ch. Weyrich, C. M. Schneider, J. Kampmeier, D. Grützmacher, L. Plucinski, M. Eschbach, and S. D. Ganichev, "Room-temperature high-frequency transport of dirac fermions in epitaxially grown Sb<sub>2</sub>Te<sub>3</sub>- and Bi<sub>2</sub>Te<sub>3</sub>-based topological insulators," *Phys. Rev. Lett.* **113**(9), 096601 (2014).
11. H. Plank, L. E. Golub, S. Bauer, V. V. Bel'kov, T. Herrmann, P. Olbrich, M. Eschbach, L. Plucinski, C. M. Schneider, J. Kampmeier, M. Lanius, G. Mussler, D. Grützmacher, and S. D. Ganichev, "Photon drag effect in (Bi<sub>1-x</sub>Sbx)<sub>2</sub>Te<sub>3</sub> three-dimensional topological insulators," *Phys. Rev. B* **93**(12), 125434 (2016).
12. P. Olbrich, E. L. Ivchenko, R. Ravash, T. Feil, S. D. Danilov, J. Allerdings, D. Weiss, D. Schuh, W. Wegscheider, and S. D. Ganichev, "Ratchet effects induced by terahertz radiation in heterostructures with a lateral periodic potential," *Phys. Rev. Lett.* **103**(9), 090603 (2009).
13. P. Olbrich, J. Kamann, M. König, J. Munzert, L. Tutsch, J. Eroms, D. Weiss, M.-H. Liu, L. E. Golub, E. L. Ivchenko, V. V. Popov, D. V. Fateev, K. V. Mashinsky, F. Fromm, Th. Seyller, and S. D. Ganichev, "Terahertz ratchet effects in graphene with a lateral superlattice," *Phys. Rev. B* **93**(7), 075422 (2016).
14. V. V. Popov, D. V. Fateev, T. Otsuji, Y. M. Meziani, D. Coquillat, and W. Knap, "Plasmonic terahertz detection by a double-grating-gate field-effect transistor structure with an asymmetric unit cell," *Appl. Phys. Lett.* **99**(24), 243504 (2011).
15. I. V. Rozhansky, V. Yu. Kachorovskii, and M. S. Shur, "Helicity-driven ratchet effect enhanced by plasmons," *Phys. Rev. Lett.* **114**(24), 246601 (2015).
16. H. Diehl, V. A. Shalygin, V. V. Bel'kov, Ch. Hoffmann, S. N. Danilov, T. Herrle, S. A. Tarasenko, D. Schuh, Ch. Gerl, W. Wegscheider, W. Prettl, and S. D. Ganichev, "Spin photocurrents in (110)-grown quantum well structures," *New J. Phys.* **9**(9), 349 (2007).
17. J. Karch, P. Olbrich, M. Schmalzbauer, C. Zoth, C. Brinsteiner, M. Fehrenbacher, U. Wurstbauer, M. M. Glazov, S. A. Tarasenko, E. L. Ivchenko, D. Weiss, J. Eroms, R. Yakimova, S. Lara-Avila, S. Kubatkin, and S. D.

- Ganichev, "Dynamic Hall effect driven by circularly polarized light in a graphene layer," *Phys. Rev. Lett.* **105**(22), 227402 (2010).
18. S. D. Ganichev, E. L. Ivchenko, S. N. Danilov, J. Eroms, W. Wegscheider, D. Weiss, and W. Prettl, "Conversion of spin into directed electric current in quantum wells," *Phys. Rev. Lett.* **86**(19), 4358–4361 (2001).
  19. C. Jiang, V. A. Shalygin, V. Yu Panevin, S. N. Danilov, M. M. Glazov, S. Rositsa Yakimova, L. Avila, S. Kubatkin, and S. D. Ganichev, "Helicity-dependent photocurrents in graphene layers excited by mid infrared radiation of a CO<sub>2</sub> laser," *Phys. Rev. B* **84**, 125429 (2011).
  20. J. E. Goff and W. L. Schaich, "Theory of the photon-drag effect in simple metals," *Phys. Rev. B* **61**(15), 10471–10477 (2000).
  21. J. E. Goff and W. L. Schaich, "Hydrodynamic theory of photon drag," *Phys. Rev. B* **56**(23), 15421–15430 (1997).
  22. S. Luryi, "Photon-drag effect in intersubband absorption by a two-dimensional electron gas," *Phys. Rev. Lett.* **58**(21), 2263–2266 (1987).
  23. V. L. Gurevich and R. Laiho, "Photomagnetism of metals, first observation of dependence on polarization of light," *Phys. Solid State* **42**(10), 1807–1812 (2000).
  24. A. S. Vengurlekar and T. Ishihara, "Surface plasmon enhanced photon drag in metal films," *Appl. Phys. Lett.* **87**(9), 091118 (2005).
  25. T. Hatano, B. Nishikawa, M. Iwanaga, and T. Ishihara, "Optical rectification effect in 1D metallic photonic crystal slabs with asymmetric unit cell," *Opt. Express* **16**(11), 8236–8241 (2008).
  26. T. Ishihara, "Optical response of semiconductor and metal-embedded photonic crystal slabs," *Phys. Status Solidi, A Appl. Res.* **201**(3), 398–404 (2004).
  27. T. Hatano, T. Ishihara, S. G. Tikhodeev, and N. A. Gippius, "Transverse photovoltage induced by circularly polarized light," *Phys. Rev. Lett.* **103**(10), 103906 (2009).
  28. H. Kurosawa and T. Ishihara, "Surface plasmon drag effect in a dielectrically modulated metallic thin film," *Opt. Express* **20**(2), 1561–1574 (2012).
  29. N. Noginova, V. Rono, F. J. Bezares, and J. D. Caldwell, "Plasmon drag effect in metal nanostructures," *New J. Phys.* **15**(11), 113061 (2013).
  30. M. M. Glazov and S. D. Ganichev, "High frequency electric field induced nonlinear effects in graphene," *Phys. Rep.* **535**(3), 101–138 (2014).
  31. M. Akbari, M. Onoda, and T. Ishihara, "Photo-induced voltage in nano-porous gold thin film," *Opt. Express* **23**(2), 823–832 (2015).
  32. M. Akbari and T. Ishihara, "Polarization dependence of transverse photo-induced voltage in gold thin film with random nanoholes," *Opt. Express* **25**(3), 2143–2152 (2017).
  33. N. V. Proscia, M. Moocarme, R. Chang, I. Kretzschmar, V. M. Menon, and L. T. Vuong, "Control of photo-induced voltages in plasmonic crystals via spin-orbit interactions," *Opt. Express* **24**(10), 10402–10411 (2016).
  34. Q. Bai, "Manipulating photoinduced voltage in metasurface with circularly polarized light," *Opt. Express* **23**(4), 5348–5356 (2015).
  35. J. D. Jackson, *Classical Electrodynamics*, 3rd ed. (John Wiley & Sons, 1999).
  36. Y. Gorodetski, N. Shitrit, I. Bretner, V. Kleiner, and E. Hasman, "Observation of optical spin symmetry breaking in nanoapertures," *Nano Lett.* **9**(8), 3016–3019 (2009).